

COMPUTATIONAL STUDIES
OF A LARGE-SCALE HYDROGEN–AIR
CONTINUOUS DETONATION COMBUSTOR**A. V. Dubrovskii^{1,2,3}, S. M. Frolov^{1,2,3}, and V. S. Ivanov^{1,2}**¹Center for Pulse Detonation Combustion
Moscow, Russia²N. N. Semenov Institute of Chemical Physics
Russian Academy of Sciences
Moscow, Russia
e-mail: smfrol@chph.ras.ru³National Research Nuclear University
“Moscow Engineering Physics Institute” (NRNU MEPhI)
Moscow, Russia

The idea of the combustion chamber with a continuous detonation was proposed by B. V. Voitsekhovskii in 1959 [1]. One of possible configurations of the continuous detonation combustor (CDC) is an annular channel formed by the walls of the two coaxial cylinders. If the bottom of the annular channel is equipped with an injector head and the other end of the channel is equipped with a nozzle, one obtains the annular jet engine. Detonative combustion in such a chamber can be arranged by starting a supply of fuel mixture through the injector head, producing a single ignition pulse for detonation initiation, and burning fuel mixture supplied through the injector head in a detonation wave (DW) continuously circulating above the chamber bottom. The DW will burn the fuel mixture newly arrived in the CDC during one revolution of the wave around the circumference of the annular channel. The rotation frequency of the DW(s) in the CDC is determined by the mean diameter of the annular gap, the mean propagation velocity of the wave, and the number of waves simultaneously rotating above the bottom. For example, in the CDC with the mean diameter of the annular gap 300 mm operating with one or two DWs propagating at 1700 m/s, the rotation

frequency will attain 1.8 or 3.6 kHz. If the fuel mixture is supplied to the CDC at the mean velocity of, say, 200 m/s, the maximum height of the fuel-mixture layer filling the CDC will be 110 or 55 mm, i. e., complete combustion in the DW(s) will be attained at a very short distance. Moreover, the combustion process in CDC can be accompanied with the total pressure rise [2]. As a matter of fact, it is shown computationally in [3] that up to 13–15 percent gain in total pressure can be readily attained in a CDC with low-pressure loss. Thus, the main advantages of such combustors include better propulsion performance due to pressure gain combustion, quasi-steady outflow of detonation products due to high-frequency cycles, short combustion chamber, simple design, and a single ignition.

In 2010–2014, our research team has developed a computational technology aimed at computer-aided design of CDC for jet engines. The technology was first successfully validated against available experimental results [4] (see [5]) and then was used for the design of our own large-scale hydrogen–air CDC. This CDC was designed, fabricated, and tested and the results of tests are reported in the complementary article [6]. Reported herein is the brief description of the technology, some results of its validation against experimental data [6] and some results of optimization studies aimed at enhancement of CDC performance.

1 Computational Technology

The physicochemical processes in the CDC are simulated using the computational technology described in detail in [7]. The flow of a viscous compressible gas in the CDC is described using the three-dimensional (3D) time-dependent Reynolds-averaged Navier–Stokes, energy, and species conservation equations for a multicomponent mixture. The turbulent fluxes of species, momentum, and energy are modeled within the framework of the two-equation turbulence model (e. g., standard k - ε model). Given that all physicochemical processes in the CDC occur in a very short time, the contribution from the frontal (laminar and/or turbulent) combustion to the chemical sources in the equations of conservation of energy and components of the mixture is neglected. The contributions of volumetric chemical reactions to chemical sources are determined using the particle method. The most important advantage

of the particle method is its ability to accurately determine the rates of chemical reactions in a turbulent flow without invoking any hypothesis about the influence of turbulent fluctuations of the temperature and concentrations of the reactants on the mean reaction rate. In the algorithm, the instantaneous local states of a turbulent reacting flow are represented as a set of interacting (Lagrangian) particles. Each particle has its own properties: the position in space, three velocity components, volume, density, temperature, mass fractions of chemical components, and statistical weight, which is used to determine the mean values of the variables over the ensemble of particles. For each particle, the system of equations of conservation of mass of the species, momentum, and energy is solved; the flux (transport) terms are calculated using the classic models of linear decay to the mean. The equations of the model are closed by the caloric and thermal equations of state of a mixture of ideal gases with variable specific heats as well as by the initial and boundary conditions. All the thermophysical parameters of the gas are considered variable.

The governing equations of the problem are solved numerically using the coupled algorithm “Semiimplicit method for pressure-linked equations (SIMPLE)–Monte Carlo method.” The chemical sources are calculated by an implicit scheme with an internal time step of integration. The coupled algorithm was previously used to simulate flame acceleration and deflagration-to-detonation transition in smooth tubes and in tubes with obstacles, as well as to solve the problems of shock-initiated autoignition and preflame ignition in confined spaces. In all cases, satisfactory agreement between the results of calculations and experiments were obtained. In addition, this algorithm was used to solve the problem of the limits of existence of detonation in the CDC operating on homogeneous hydrogen–air mixture.

2 Continuous Detonation Combustor

2.1 Baseline configuration

The baseline configuration of the CDC has been obtained as a result of extended preliminary computational studies with hydrogen and air as fuel components. This baseline configuration was then used for the design of an experimental CDC. Thereafter, the experimental CDC was

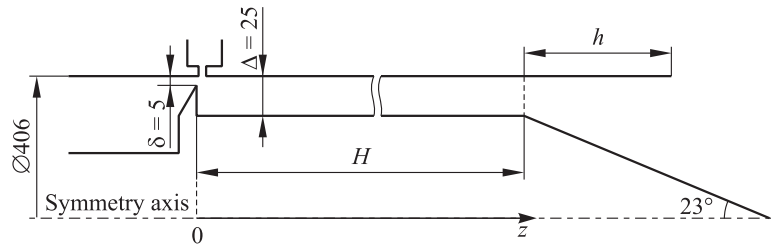


Figure 1 Continuous detonation combustor. Dimensions are in millimeters

fabricated and tested to validate the computational predictions in terms of different qualitative and quantitative features (existence of the detonation mode, mass flow rates of air and hydrogen, detonation wave velocity and height, the number of simultaneously rotating detonation waves, thrust, specific impulse, etc.). The results of experiments are discussed in detail in the complimentary article [6]. In this subsection, the predictive capabilities of the computational technology outlined in section 1 are demonstrated by comparing some predicted and measured results for the CDC of baseline configuration.

Figure 1 shows a schematic of the CDC of baseline configuration with the dimensions of its key elements. The combustion chamber is an axisymmetric annular channel with the external diameter of the annular gap 406 mm, gap width 25 mm, and length 310 mm. The axial distance is measured from the CDC bottom ($z = 0$). Between the bottom and the outer wall of the CDC, there is an annular slit of width $\delta = 5$ mm for air supply in the axial direction from an air plenum. Hydrogen enters the CDC from a hydrogen plenum in the radial direction through 240 nozzles evenly spaced over the circumference of the chamber's outer wall $z = 1$ mm apart. The total cross-sectional area of the nozzles is 1.9 cm^2 . The right end of the CDC is open to the environment via an outlet nozzle with a conical center body. The half-angle of the cone is 23° . The other essential part of the nozzle is its outer extension of length $h = 295$ mm.

The values of static pressure in air and hydrogen manifolds are taken equal to 4 and 18 atm, respectively. The calculated mass flow rates of air and hydrogen in the CDC at these conditions are 6.4 and

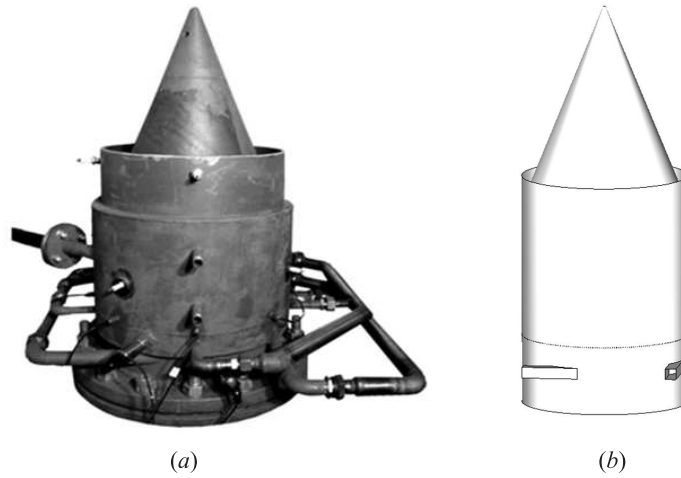


Figure 2 Experimental (a) and computational (b) models of the CDC

0.26 kg/s, respectively, which corresponds to overall hydrogen-rich composition with the fuel–air equivalence ratio of 1.4.

Figure 2 shows the experimental (see Fig. 2a) and computational (see Fig. 2b) CDC of baseline configuration. It is seen from Fig. 2a that in the experimental CDC, air is supplied to the chamber through four side tubes of round cross section connected to the outer CDC wall tangentially. In the computational CDC, the round tubes are replaced by the channels of square cross section of the same area. Also seen in Fig. 2b is the belt of multiple nozzles for hydrogen injection equally distributed along the circumference of the chamber’s outer wall.

The calculations of the CDC of baseline configuration were performed on 192 CPUs using the structured computational mesh containing about 2,600,000 hexagonal cells with cell size compression in the regions of mixing and reaction. The minimum cell size was 0.5 mm.

Figure 3 shows the predicted snapshots of temperature, static pressure, mass fraction of hydrogen, and flow Mach number near the outer wall of the CDC of baseline configuration operating in the continuous detonation mode with one DW. The upper and lower rows of the snapshots in Fig. 3 correspond to two time instants after ignition: 7.65 and

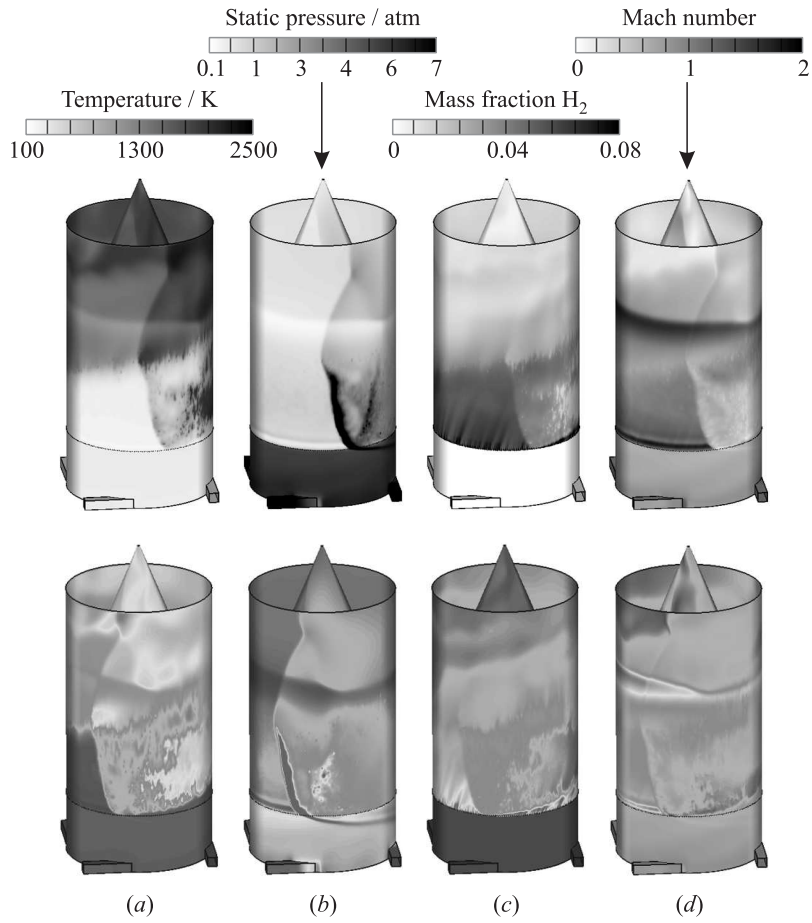


Figure 3 Predicted snapshots of temperature (*a*), static pressure (*b*), mass fraction of hydrogen (*c*), and flow Mach number (*d*) near the outer wall of the CDC of baseline configuration operating in the continuous detonation mode with one DW at air and hydrogen supply pressures 4 and 18 atm. Detonation propagates from right to left: upper row — 7.65 ms after ignition, and lower row — 7.75 ms after ignition. (Refer color plate, p. XI.)

7.75 ms, respectively. Some specific features of the flow pattern in the CDC are worth mentioning. First, the reaction zone behind the propagating detonation wave is highly nonuniform (see Fig. 3*a*) and exhibits strong transverse shock waves (see Fig. 3*b*). Second, the mixture composition in front of the propagating detonation is highly nonuniform (see Fig. 3*c*). Third, an intense bow shock penetrates in the air manifold (see Fig. 3*b*) but this bow shock does not induce the backflow of reactive mixture and detonation products in the air manifold (see Figs. 3*c* and 3*a*). Fourth, the height of the DW is about 200–220 mm, i.e., about 8–9

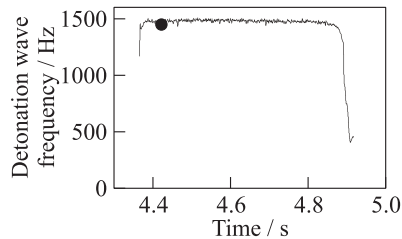


Figure 4 Predicted (point) and measured (curve) frequencies of detonation rotation in the CDC of baseline configuration with air and hydrogen supply pressures 4 and 18 atm

times the gap width (25 mm) (see Figs. 3*a* and 3*b*). Finally, the flow of detonation products becomes supersonic slightly above the DW, passes through the Mach disk, and becomes subsonic but highly nonuniform in the outlet nozzle (see Fig. 3*d*). The latter indicates that the nozzle in the CDC of baseline configuration is not optimized.

Figure 4 compares the predicted (point) detonation rotation frequency in the CDC with the experimental curve for similar initial and boundary conditions in terms of the air and hydrogen supply pressures (4 and 18 atm). Both in calculations and in experiment, the operation mode with one rotating DW with a very similar rotation frequency (1460–1490 Hz) is obtained. This rotation frequency corresponds to the detonation propagation velocity 1860 m/s which is close to the thermodynamic detonation velocity in the stoichiometric hydrogen–air mixture (~ 1970 m/s) but is lower than the thermodynamic detonation velocity for fuel-rich hydrogen–air mixture with the equivalence ratio of 1.4 (~ 2065 m/s).

Figure 5 compares the predicted thrust level (point) of the CDC with the measured thrust curve in the same computational and experimental runs as in Fig. 4. Note that Fig. 5 shows the full thrust produced by both air and hydrogen blowdown process and by a detonative combustion. As is seen, the predicted thrust level of 4.5 kN agrees within

times the gap width (25 mm) (see Figs. 3*a* and 3*b*). Finally, the flow of detonation products becomes supersonic slightly above the DW, passes through the Mach disk, and becomes subsonic but highly nonuniform in the outlet nozzle (see Fig. 3*d*). The latter indicates that the nozzle in the CDC of baseline configuration is not optimized.

Figure 4 compares the predicted (point) detonation rotation frequency in the CDC with the experimental curve for similar initial and boundary conditions in terms of the air and hydrogen supply pressures (4 and 18 atm).

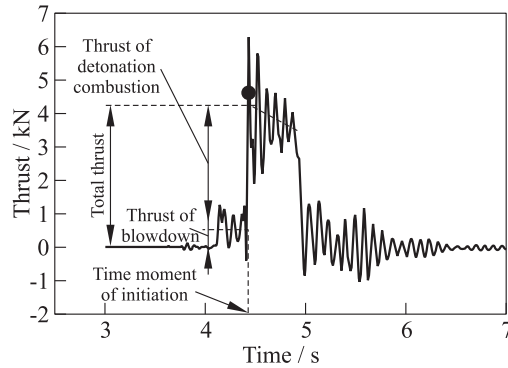


Figure 5 Predicted (point) and measured (curve) thrust produced by the CDC of baseline configuration with air and hydrogen supply pressures 4 and 18 atm

7% with the measured value of ~ 4.3 kN at the onset of detonative combustion in the CDC. Note that the calculations were made for the fixed values of static pressures of air and hydrogen in manifolds, whereas in the course of the experiment, these values slightly decayed resulting in the decrease of thrust (see the descending dashed line in Fig. 5). Note also that in the calculations, the thrust was determined as the integral pressure force acting on all rigid surfaces of the CDC, i. e., viscous forces were not taken into account. The account of viscous friction at rigid walls will inevitably decrease the predicted thrust level but not much.

2.2 Effect of continuous detonation combustor height on thrust

Discussed in this subsection are the results of calculations aimed at determining the effect of CDC height on the calculated thrust, other conditions being equal. Table 1 presents three test cases with three different values of CDC height, namely, 155, 310 (baseline), and 465 mm, and Fig. 6 shows the corresponding CDC pictures. As is seen from Table 1, despite in all three cases the CDC operates in the detonative mode with one continuously rotating DW, the highest thrust is

Table 1 Test cases with three different values of CDC height

Run	H , mm	Overall equivalence ratio	\dot{m}_{air} , kg/s	\dot{m}_{H_2} , kg/s	Combustion mode	Thrust (calc.), kN
1	155	1.4	6.4	0.26	1 DW	3.7
2*	310	1.4	6.4	0.26	1 DW	4.5
3	465	1.4	6.4	0.26	1 DW	4.3

*Baseline configuration

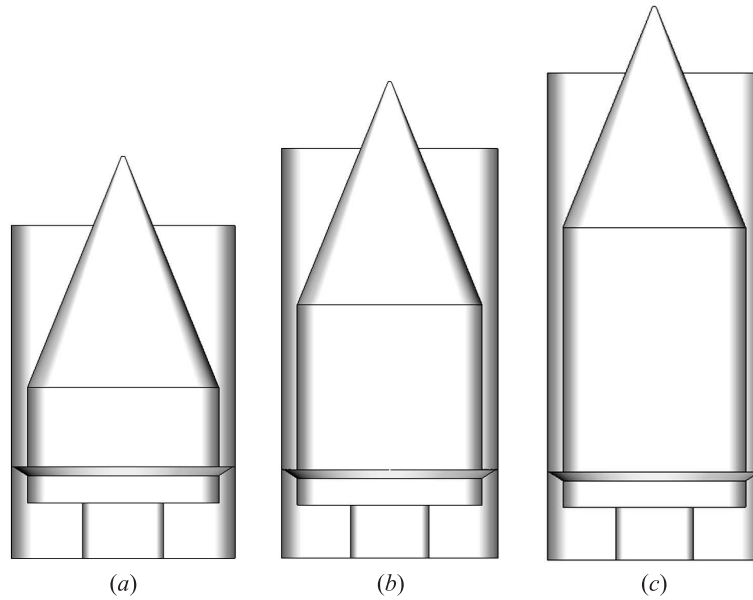


Figure 6 Test cases with three different values of CDC height H : (a) 155 mm; (b) 310; and (c) 465 mm

obtained in the CDC of baseline configuration. Decrease of the CDC height by 155 mm from 310 mm results in thrust decrease by 18% and increase of the CDC height by 155 mm from 310 mm results in thrust decrease by 4%. This indicates that the height of the CDC of baseline configuration is nearly optimal.

2.3 Effect of overall equivalence ratio on thrust

Discussed in this subsection are the results of calculations aimed at determining the effect of mass flow rate of hydrogen on the calculated thrust, other conditions being equal. In this series of calculations, the height of the CDC (H) was taken equal to 395 mm and the length of nozzle extension (h) was taken equal to 0, i.e., the annual gap terminates at the cone base. Table 2 and Fig. 7 present four test cases with four different values of the overall equivalence ratio, namely, 0.55, 0.8, 1.0, and 1.4 obtained by variation of mass flow rate of hydrogen from 0.1 to 0.26 kg/s. The mean thrust was estimated on time interval Δt as shown in Fig. 7. As is seen from Table 2, at fuel-lean overall equivalence ratios (0.55 and 0.8), no stable operation mode was obtained in the calculations. At equivalence ratio 0.55, the reaction zone was blown off from the CDC thus producing no thrust, whereas at equivalence ratio 0.8, the unsteady combustion mode was observed producing highly irregular thrust. At overall equivalence ratios 1.0 and 1.4, a stable operation mode of the CDC with one DW was obtained. In these test cases, the thrust level was 6.1 and 6.5 kN, respectively. Comparison of Run 2 in Table 1 and Run 7 in Table 2 indicates that truncation of nozzle extension length from $h = 295$ to 0 mm results in a considerable CDC thrust increase (from 4.5 to 6.1 kN), other conditions been equal. Contrary to Run 2 (baseline CDC configuration), where the flow becomes subsonic after passing through a strong Mach disc inside the CDC, the supersonic flow in Run 7 passes through a weak Mach disc located well outside the exit plane of the CDC and remains mostly supersonic.

Table 2 Test cases with four different values of overall equivalence ratio

Run	H , mm	Overall equivalence ratio	\dot{m}_{air} , kg/s	\dot{m}_{H_2} , kg/s	Combustion mode	Thrust (calc.), kN
4	395	0.55	6.4	0.1	Blow off	0.35
5	395	0.8	6.4	0.144	Unsteady	2.25
6	395	1.0	6.4	0.18	1 DW	6.1
7	395	1.4	6.4	0.26	1 DW	6.5

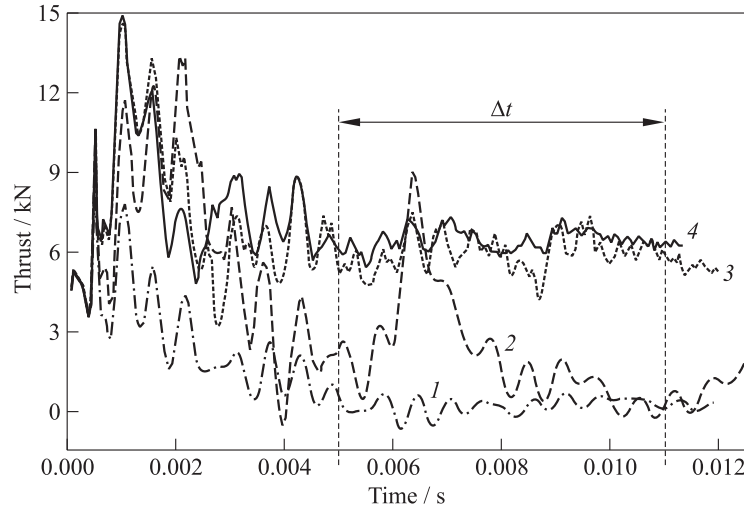


Figure 7 Predicted time histories of thrust produced by the CDC at different overall equivalence ratios (φ is the fuel-air equivalence ratio and Δt is the time interval for estimating the CDC thrust): 1 — $\varphi = 0.55$; 2 — 0.8; 3 — 1.0; and 4 — $\varphi = 1.4$

3 Concluding Remarks

The computational technology for computer-aided design of jet engines operating on continuous detonations has been applied to design a large-scale hydrogen-air CDC of outer diameter 406 mm and total mass flow rate of fuel mixture up to 7 kg/s. Thereafter, the experimental CDC was fabricated and tested to validate the computational predictions in terms of different qualitative and quantitative features (existence of the detonation mode, mass flow rates of air and hydrogen, detonation wave velocity and height, the number of simultaneously rotating detonation waves, thrust, specific impulse, etc.).

It appeared that the computational technology taking into account finite-rate chemistry of hydrogen oxidation and turbulence-chemistry interaction provides excellent agreement with experimental data and can be used for design optimization aimed at the improvement of CDC propulsion performance.

Acknowledgments

This work was partially supported by the Program #26 “Combustion and Explosion” of the Presidium of the Russian Academy of Sciences.

References

1. Voitsekhovskii, B. V. 1959. Stationary detonation. *Dokl. USSR Acad. Sci.* 129:1254–1256.
2. Zel’dovich, Ya. B. 1940. To the question of energy use of detonation combustion. *Zh. Tekhn. Fiz.* 10(17):1453–1461. [In Russian.]
3. Frolov, S. M., A. V. Dubrovsky, and V. S. Ivanov. 2013. Three-dimensional numerical simulation of a continuously rotating detonation in the annular combustion chamber with a wide gap and separate delivery of fuel and oxidizer. *5th EUCASS Proceedings*. Munich, Germany. Paper P197.
4. Bykovskii, F. A., S. A. Zhdan, and E. F. Vedernikov. 2006. Continuous spin detonation of fuel–air mixtures. *Combust. Expl. Shock Waves* 42(4):1–9.
5. Frolov, S. M., A. V. Dubrovskii, and V. S. Ivanov. 2013. Three-dimensional numerical simulation of the operation of a rotating-detonation chamber with separate supply of fuel and oxidizer. *Russ. J. Phys. Chem. B* 7(1): 35–43.
6. Frolov, S. M., V. S. Aksenov, V. S. Ivanov, S. N. Medvedev, and I. O. Shamshin. 2014. Experimental studies of a large-scale hydrogen–air continuous detonation combustor. In: *Transient combustion and detonation phenomena*. Eds. S. M. Frolov and G. D. Roy. Moscow: TORUS PRESS. 449–465.
7. Frolov, S. M., A. V. Dubrovskii, and V. S. Ivanov. 2012. Three-dimensional numerical simulation of the operation of the rotating detonation chamber. *Russ. J. Phys. Chem. B* 6(2):276–288.